Provided for non-commercial research and education use.
Not for reproduction, distribution or commercial use.

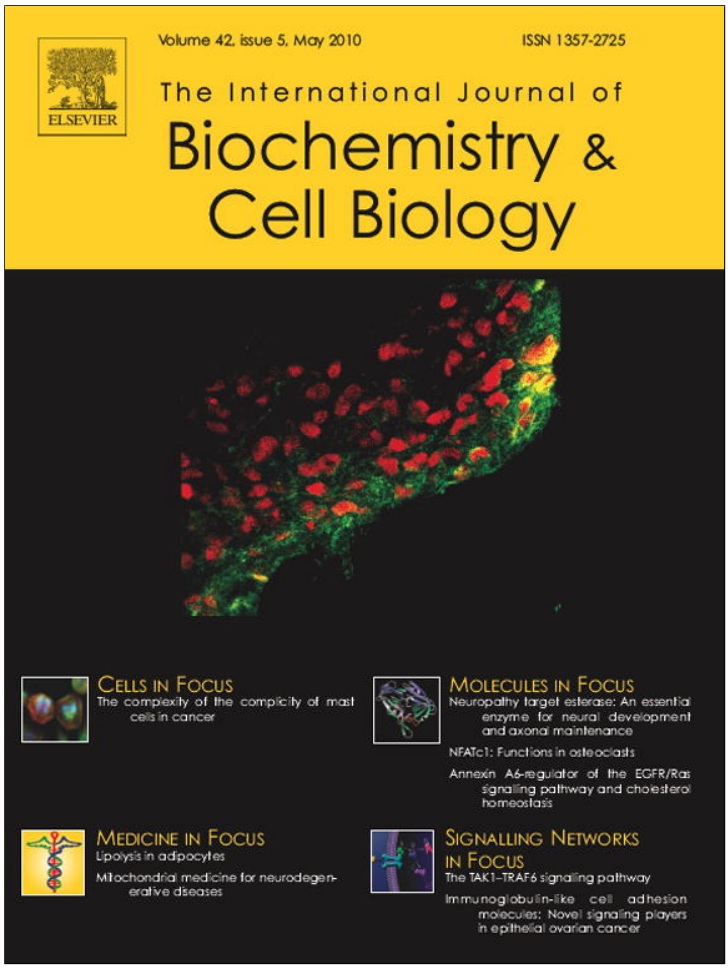

This article appeared in a journal published by Elsevier. The attached copy is furnished to the author for internal non-commercial research and education use, including for instruction at the authors institution and sharing with colleagues.

Other uses, including reproduction and distribution, or selling or licensing copies, or posting to personal, institutional or third party websites are prohibited.

In most cases authors are permitted to post their version of the article (e.g. in Word or Tex form) to their personal website or institutional repository. Authors requiring further information regarding Elsevier's archiving and manuscript policies are encouraged to visit:

http://www.elsevier.com/copyright

Author's personal copy

The International Journal of Biochemistry & Cell Biology 42 (2010) 712–724

Contents lists available at ScienceDirect

The International Journal of Biochemistry & Cell Biology

journal homepage: www.elsevier.com/locate/biocel

Inhibitory mechanisms and binding site location for serotonin selective reuptake inhibitors on nicotinic acetylcholine receptors

Hugo R. Arias[a,*], Dominik Feuerbach[b], Pankaj Bhumireddy[c], Marcelo O. Ortells[d]

[a] Department of Pharmaceutical Sciences, College of Pharmacy, Midwestern University, 19555 N. 59th Ave Glendale, AZ, USA
[b] Neuroscience Research, Novartis Institutes for Biomedical Research, Basel, Switzerland
[c] Department of Pharmaceutical Sciences, College of Pharmacy, Western University of Health Sciences, Pomona, CA, USA
[d] Faculty of Medicine and CONICET, University of Morón, Argentina

ARTICLE INFO

Article history:
Received 3 November 2009
Received in revised form
22 December 2009
Accepted 6 January 2010
Available online 14 January 2010

Keywords:
Nicotinic acetylcholine receptors
Serotonin selective reuptake inhibitors
Conformational states
Ca^{2+} influx
Radioligand binding
Molecular modeling

ABSTRACT

Functional and structural approaches were used to examine the inhibitory mechanisms and binding site location for fluoxetine and paroxetine, two serotonin selective reuptake inhibitors, on nicotinic acetylcholine receptors (AChRs) in different conformational states. The results establish that: (a) fluoxetine and paroxetine inhibit hα1β1γδ AChR-induced Ca^{2+} influx with higher potencies than dizocilpine. The potency of fluoxetine is increased ~10-fold after longer pre-incubation periods, which is in agreement with the enhancement of [^{3}H]cytisine binding to resting but activatable *Torpedo* AChRs elicited by these antidepressants, (b) fluoxetine and paroxetine inhibit the binding of the phencyclidine analog piperidyl-3,4-^{3}H(N)]-(N-(1-(2 thienyl)cyclohexyl)-3,4-piperidine to the desensitized *Torpedo* AChR with higher affinities compared to the resting AChR, and (c) fluoxetine inhibits [^{3}H]dizocilpine binding to the desensitized AChR, suggesting a mutually exclusive interaction. This is supported by our molecular docking results where neutral dizocilpine and fluoxetine and the conformer of protonated fluoxetine with the highest LUDI score interact with the domain between the valine (position 13′) and leucine (position 9′) rings. Molecular mechanics calculations also evidence electrostatic interactions of protonated fluoxetine at positions 20′, 21′, and 24′. Protonated dizocilpine bridges these two binding domains by interacting with the valine and outer (position 20′) rings. The high proportion of protonated fluoxetine and dizocilpine calculated at physiological pH suggests that the protonated drugs can be attracted to the channel mouth before binding deeper within the AChR ion channel between the leucine and valine rings, a domain shared with phencyclidine, finally blocking ion flux and inducing AChR desensitization.

© 2010 Elsevier Ltd. All rights reserved.

1. Introduction

Nicotinic acetylcholine receptors (AChRs) are members of the Cys-loop ligand-gated ion channel superfamily that also includes types A and C γ-aminobutyric acid, type 3 serotonin, and glycine receptors (reviewed in Arias, 2006; Albuquerque et al., 2009). AChR function can be modulated by a wide range of structurally different molecules that interact with the ion channel, the so-called noncompetitive antagonists (NCAs). Among the clinically important NCAs are structurally and functionally different antidepressants (reviewed in Arias et al., 2006a; Arias, 2009). The inhibitory action elicited by antidepressants on AChRs supports the cholinergic–adrenergic hypothesis, which states that hyperactivity or hypersensitivity of the cholinergic system over the adrenergic system can lead to depressed mood states (reviewed in Shytle et al., 2002). In this regard, the therapeutic action of many antidepressants may be mediated in part through inhibition of one or more AChRs.

Serotonin selective reuptake inhibitors (SSRIs) (see molecular structures in Fig. 1) are one of the most widely used antidepressants and inhibit different AChRs in a noncompetitive fashion (García-Colunga et al., 1997, 2004; Maggi et al., 1998; López-Valdés and García-Colunga, 2001; García-Colunga and Miledi, 1999; Fryer and

Abbreviations: AChR, nicotinic acetylcholine receptor; NCA, noncompetitive antagonist; PCP, phencyclidine; dizocilpine, (5R,10S)-(+)-5-methyl-10,11-dihydro-5H-dibenzo[a,d]cyclohepten-5,10-imine hydrogen maleate; fluoxetine, (±)-*N*-methyl-γ-(4-(trifluoromethyl)phenoxy)benzenepropanamine; paroxetine, (3S-trans)-3-[(1,3-benzodioxol-5-yloxy)methyl]-4-(4-fluorophenyl)piperidine; [^{3}H]TCP, piperidyl-3,4-3H(*N*)]-(*N*-(1-(2 thienyl)cyclohexyl)-3,4-piperidine; CCh, carbamylcholine; α-BTx, α-bungarotoxin; RT, room temperature; BS buffer, binding saline buffer; K_i, inhibition constant; K_d, dissociation constant; IC_{50}, ligand concentration that produces 50% inhibition of binding or of ion flux; EC_{50}, ligand concentration that produces 50% increase of binding or of ion flux; n_H, Hill coefficient; PMSF, phenylmethylsulfonyl fluoride; DMEM, Dulbecco's Modified Eagle Medium; BSA, bovine serum albumin; FLIPR, fluorescent imaging plate reader; RMS, root mean square.

* Corresponding author. Tel.: +1 623 572 3589; fax: +1 623 572 3550.
E-mail address: harias@midwestern.edu (H.R. Arias).

1357-2725/$ – see front matter © 2010 Elsevier Ltd. All rights reserved.
doi:10.1016/j.biocel.2010.01.007

Author's personal copy

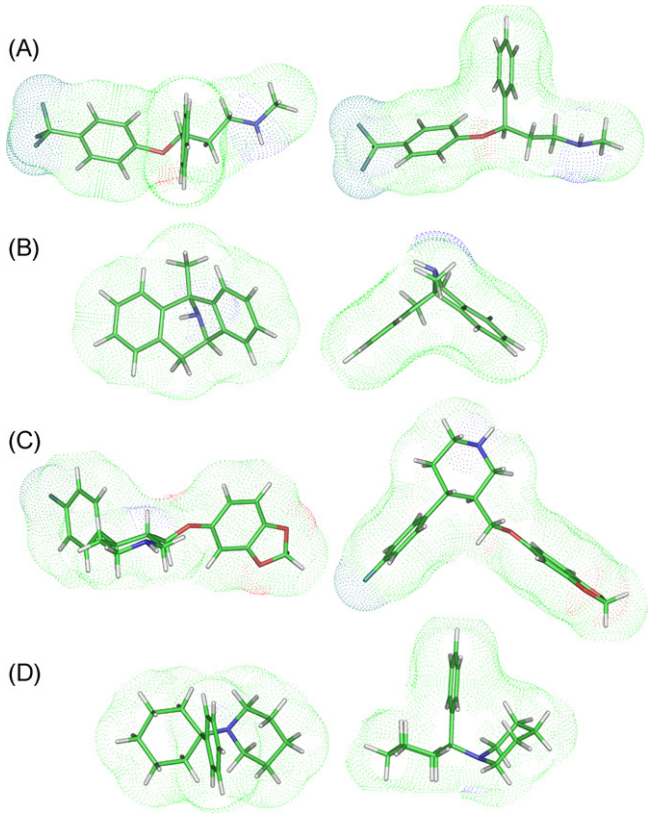

Fig. 1. Molecular structure of (A) fluoxetine, (B) dizocilpine, (C) paroxetine, and (D) phencyclidine (PCP). Molecules are in stick representation and surrounded by their calculated accessible surface.

Lukas, 1999). However, we do not have a thorough understanding of how these antidepressants (i.e., fluoxetine and paroxetine) interact with the ion channel when the AChR is in different conformational states. As a first attempt to study this interaction we chose the muscle-type AChR because it is the archetype of the Cys-loop ligand-gated ion channel superfamily and because we can manipulate the different receptor conformational states in a variety of *in vitro* assays. Moreover, the muscle-type AChR is the target for the therapeutical action of fluoxetine when it is used for the treatment of slow-channel congenital myasthenic syndrome, an autosomal dominant disorder caused by gain-of-function mutations in this AChR subtype (Harper et al., 2003; reviewed in Harper, 2004). We also used the muscle-type AChR because the binding site locations of several NCAs have already been characterized (reviewed in Arias et al., 2006a), including that for phencyclidine (PCP) (Arias et al., 2002, 2003, 2006b; Sanghvi et al., 2008; Hamouda et al., 2008; Eaton et al., 2000), and dizocilpine (see molecular structures in Fig. 1) (Arias et al., 2001). Taking advantage of this previous knowledge, the localization of the SSRI binding sites relative to these NCAs will be determined. To accomplish these objectives, we will use structural and functional approaches including radioligand competition binding assays using radiolabeled ligands such as [piperidyl-3,4-^{3}H(*N*)]-*N*-(1-(2 thienyl)cyclohexyl)-3,4-piperidine ([^{3}H]TCP, a PCP analog) [^{3}H]dizocilpine, and the agonist [^{3}H]cytisine, as well as Ca^{2+} influx assays, and molecular modeling and docking studies.

Although this study does not intend to determine the therapeutic properties of SSRIs, the results from this work will pave the way for a better understanding of how these compounds interact with the AChR ion channel in different conformational states and subsequently, novel NCAs with antidepressant activity might be developed.

2. Materials and methods

2.1. Materials

[Piperidyl-3,4-^{3}H(*N*)]-(*N*-(1-(2 thienyl)cyclohexyl)-3,4-piperidine) ([^{3}H]TCP; 45 Ci/mmol), (+)-[3-^{3}H]dizocilpine (21.7 Ci/mmol), [^{3}H]cytisine hydrochloride (35.6 Ci/mmol), and [^{3}H]nicotine (77 Ci/mmol), were obtained from PerkinElmer Life Sciences Products, Inc. (Boston, MA, USA), and stored in ethanol at −20 °C. Phencyclidine hydrochloride (PCP) was obtained through the National Institute on Drug Abuse (NIDA) (NIH, Baltimore, MA, USA). Fluoxetine [(±)-*N*-methyl-γ-(4-(trifluoromethyl)phenoxy)benzenepropanamine] hydrochloride, paroxetine [(3S-trans)-3-[(1,3-benzodioxol-5-yloxy)methyl]-4-(4-fluorophenyl)piperidine] hydrochloride hemihydrate, carbamylcholine chloride (CCh), proadifen hydrochloride, suberyldicholine dichloride, (±)-epibatidine, bovine serum albumin (BSA), phenylmethylsulfonyl fluoride (PMSF), and polyethylenimine were purchased from Sigma Chemical Co. (St. Louis, MO, USA). (+)-Dizocilpine maleate and (−)-cytisine were obtained from Tocris Bioscience (Ellisville, MO, USA). α-Bungarotoxin (α-BTx) was obtained from Invitrogen Co. (Carlsbad, CA, USA). [1-(Dimethylamino) naphtalene-5-sulfonamido]ethyltrimethylammonium perchlorate (dansyltrimethylamine) was purchased from Pierce Chemical Co. (Rockford, IL, USA). Fetal bovine serum and trypsin/EDTA were purchased form Gibco BRL (Paisley, UK). Salts were of analytical grade.

2.2. Preparation of Torpedo AChR native membranes

AChR native membranes were prepared from frozen *Torpedo californica* electric organs obtained from Aquatic Research Consultants (San Pedro, CA, USA) by differential and sucrose density gradient centrifugation, as described previously (Pedersen et al., 1986). Total AChR membrane protein was determined by using the bicinchoninic acid protein assay (Thermo Fisher Scientific, Rockford, IL, USA). Specific activities of these membrane preparations were determined by the decrease in dansyltrimethylamine (6.6 μM) fluorescence produced by the titration of suberyldicholine into receptor suspensions (0.3 mg/mL) in the presence of 100 μM PCP and ranged from 1.0 to 1.2 nmol of suberyldicholine binding sites/mg total protein (0.5–0.6 nmol AChR/mg protein). The AChR membrane preparations were stored at −80 °C in 20% sucrose.

2.3. TE671 cells expressing human fetal muscle AChRs

The TE671 cell line is a human rhabdomyosarcoma cell line (obtained from American Type Culture Collection, USA) that endogenously expresses the human fetal muscle AChR (i.e., α1β1γδ). TE671 cells were cultured in a 1:1 mixture of Dulbecco's Modified Eagle Medium (DMEM) and Ham's F-12 Nutrient Mixture (Seromed Biochrom, Berlin, Germany), supplemented with 10% (v/v) fetal bovine serum, as previously described (Michelmore et al., 2002; Arias et al., 2009). DMEM/Ham's F-12 contains 1.2 g/L $NaHCO_3$, 3.2 g/L sucrose, and stable glutamine (L-Alanyl-L-Glutamine, 524 mg/L). The cells were incubated at 37 °C, 5% CO_2 and 95% relative humidity. The cells were passaged every 3 days by detaching the cells from the cell culture flask by washing with phosphate-buffered saline and brief incubation (~3 min) with trypsin (0.5 mg/mL)/EDTA (0.2 mg/mL).

2.4. Ca^{2+} influx measurements in TE671 cells

Ca^{2+} influx was determined as previously described (Michelmore et al., 2002; Arias et al., 2009). Briefly, 5×10^4

Author's personal copy

TE671 cells per well were seeded 72 h prior to the experiment on black 96-well plates (Costar, Corning Inc., New York, USA) and incubated at 37 °C in a humidified atmosphere (5% CO_2/95% air). 16–24 h before the experiment, the medium was changed to 1% BSA in HEPES-buffered salt solution (HBSS) (130 mM NaCl, 5.4 mM KCl, 2 mM $CaCl_2$, 0.8 mM $MgSO_4$, 0.9 mM NaH_2PO_4, 25 mM glucose, 20 mM HEPES, pH 7.4). On the day of the experiment, the medium was removed by flicking the plates and replaced with 100 μL HBSS/1% BSA containing 2 mM Fluo-4 (Molecular Probes, Eugene, OR, USA) in the presence of 2.5 mM probenecid (Sigma, Buchs, Switzerland). The cells were then incubated at 37 °C in a humidified atmosphere (5% CO_2/95% air) for 1 h. Plates were flicked to remove excess of Fluo-4, washed twice with HBSS/1% BSA, and finally refilled with 100 μL of HBSS containing different ligand concentrations, and pre-incubated for 5 min (and for 4 and 24 h in the case of fluoxetine). Plates were then placed in the cell plate stage of the fluorescent imaging plate reader (FLIPR) (Molecular Devices, Sunnyvale, CA, USA). A baseline consisting of 5 measurements of 0.4 s each was recorded. (±)-Epibatidine (1 μM) was then added from the agonist plate (placed in the agonist plate stage of the FLIPR) to the cell plate using the FLIPR 96-tip pipettor simultaneously to fluorescence recordings for a total length of 3 min. The laser excitation and emission wavelengths are 488 and 510 nm, at 1 W, and a CCD camera aperture of 0.4 s.

2.5. Radioligand binding experiments using Torpedo AChRs in different conformational states

We studied the influence of fluoxetine and paroxetine on [^{3}H]TCP and [^{3}H]dizocilpine binding to *Torpedo* AChRs in different conformational states. In this regard, *Torpedo* AChR native membranes (0.3 μM) were suspended in binding saline (BS) buffer (50 mM Tris–HCl, 120 mM NaCl, 5 mM KCl, 2 mM $CaCl_2$, 1 mM $MgCl_2$, pH 7.4) with 6.5 nM [^{3}H]TCP or with 20 nM [^{3}H]dizocilpine in the presence of 1 mM CCh (desensitized/CCh-bound state), or alternatively with 9.2 nM [^{3}H]TCP in the presence of 1 μM α-BTx (resting/α-BTx-bound state), and pre-incubated for 30 min at RT. α-Bungarotoxin is a competitive antagonist that maintains the AChR in the resting (closed) state (Moore and McCarthy, 1995). For the [^{3}H]TCP competition experiments, nonspecific binding was determined in the presence of 50 μM PCP (desensitized/CCh-bound state experiments), or in the presence of 100 μM PCP (resting/α-BTx-bound state experiments), as was used previously (Arias et al., 2002, 2003, 2006b, 2009; Gumilar et al., 2003). For the [^{3}H]dizocilpine competition experiments, nonspecific binding was determined in the presence of 400 μM dizocilpine according to the [^{3}H]dizocilpine K_d (4.8 μM; Arias et al., 2001).

To determine whether SSRIs modulate agonist binding to *Torpedo* AChRs in different conformational states, AChR membranes (0.3 μM) were incubated with 7.7 nM [^{3}H]cytisine in the absence (the resting but activatable state predominates) or in the presence of 200 μM proadifen (the desensitized state predominates). The local anesthetic proadifen is a potent desensitizing agent that does not interact directly with the agonist sites (Aracava and Albuquerque, 1984). To determine the affinity of cytisine for the resting and desensitized *Torpedo* AChRs, AChR membranes (0.3 μM) were incubated with 6.9 nM [^{3}H]nicotine in the absence (the resting state predominates) or in the presence of 200 μM proadifen (the desensitized state predominates). The nonspecific binding was determined in the presence 1 mM CCh.

The total volume was divided into aliquots, and increasing concentrations of the ligand under study were added to each tube and incubated for 2 h at RT. AChR-bound radioligand was then separated from free radioligand by a filtration assay using a 48-sample harvester system with GF/B Whatman filters (Brandel Inc., Gaithersburg, MD, USA), previously soaked with 0.5% polyethylenimine for 30 min. The membrane-containing filters were transferred to scintillation vials with 3 mL of Bio-Safe II (Research Product International Corp, Mount Prospect, IL, USA), and the radioactivity was determined using a Beckman LS6500 scintillation counter (Beckman Coulter, Inc., Fullerton, CA, USA).

The concentration-response data were curve-fitted by nonlinear least-squares analysis using the Prism software (GraphPad Software, San Diego, CA). The corresponding IC_{50} values were calculated using the following equation:

$$\theta = 1/[l + ([L]/IC_{50})^{n_H}] \quad (1)$$

where θ is the fractional amount of the radioligand bound in the presence of inhibitor at a concentration [L] compared to the amount of the radioligand bound in the absence of inhibitor (total binding). IC_{50} is the inhibitor concentration at which $\theta = 0.5$ (50% bound), and n_H is the Hill coefficient. The n_H values were summarized in Table 2.

The observed IC_{50} values from the competition experiments described above were transformed into inhibition constant (K_i) values using the Cheng–Prusoff relationship (Cheng and Prusoff, 1973):

$$K_i = IC_{50}/\{1 + ([\text{ligand}]/K_d^{\text{ligand}})\} \quad (2)$$

where [ligand] is the initial concentration of [^{3}H]TCP, [^{3}H]dizocilpine, and [^{3}H]nicotine, respectively, and K_d^{ligand} is the dissociation constant for [^{3}H]TCP [0.83 μM in the resting state (Arias et al., 2003), and 0.25 μM in the desensitized state (Pagán et al., 2001)], [^{3}H]dizocilpine (4.8 μM in the desensitized state; Arias et al., 2001), and [^{3}H]nicotine [0.6 μM in the resting state and 0.22 μM in the desensitized state (Middleton and Cohen, 1991)].

2.6. Schild-type analysis for dizocilpine-induced inhibition of [^{3}H]TCP binding

In order to have a better indication whether dizocilpine inhibits [^{3}H]TCP binding to the desensitized AChR by a steric or allosteric mechanism, dizocilpine-induced inhibition of [^{3}H]TCP binding experiments were performed with a initial concentration of [^{3}H]TCP and increasing concentrations of unlabeled PCP (i.e., 0, 3.1, 6.6, and 9.6 μM, respectively). The rationale of this experiment is based on the expectation that, for a higher initial concentration of the radioligand, a higher concentration of the competitor will be necessary to produce a total inhibition of radioligand binding. This is consistent with Schild-type analysis (Schild, 1949). From these competition curves the apparent IC_{50} values were obtained from the plots according to Eq. (1). Then, the ratio between the IC_{50} values for dizocilpine determined at different initial concentrations of unlabeled PCP under the IC_{50} control values (no PCP added) *versus* the initial PCP concentration ($IC_{50}^{PCP}/IC_{50}^{control}$ *versus* $[PCP]_{initial}$) (for more details see Arias et al., 2002) was plotted. A linear relationship from this modified Schild-type plot would indicate a competitive interaction, whereas a nonlinear relationship would suggest an allosteric mechanism of inhibition (Schild, 1949; Arias et al., 2002).

2.7. Molecular docking of fluoxetine and dizocilpine in the Torpedo AChR ion channel

The electron microscopy structure of the *Torpedo* AChR (Miyazawa et al., 2003; Unwin, 2005) determined at ~4 Å resolution (PDB entry 2BG9) was used as a starting point in the molecular simulations. Following the methodology of a previous work (Ortells and Barrantes, 2002), an automatic docking procedure was employed to investigate the binding modes of fluoxetine and dizocilpine in their neutral and protonated states in this modeled receptor. Subsequently, theoretical estimations of their affinities to

Author's personal copy

the *Torpedo* AChR ion channel model were carried out. More specifically, the *Torpedo* AChR structure was energy minimized using molecular mechanics (Keserü and Kolossváry, 1999) in two steps, using the program Discover and the CVFF force field (Discover, 2000; Molecular Simulations Inc., San Diego, CA, USA) (Doucet and Weber, 1996). First, energy minimization was carried out fixing the backbone atoms to their original positions, to avoid distorting the secondary structure. Second, the structure was minimized using the steepest descents method until the maximum derivative was less than 2.00 kcal $Å^{-1}$, with no Morse functions and no cross terms. The model was further minimized with the conjugate gradients method until the maximum derivative was less than 0.05 kcal $Å^{-1}$, also fixing the backbone atoms, but using the full model, with Morse functions and cross terms.

Fluoxetine and dizocilpine, in their neutral and protonated states, were first modeled using the Insight II software (InsightII, 2000; Molecular Simulations Inc., San Diego, CA, USA). Minimization and partial charge calculations were done using the MOPAC program as implemented in Insight II and employing the semiempirical AM1 method. Parameters for the electronic state were set to: lowest electronic state, Hamiltonian spin restricted, and null total charge. All other parameters were left with default values. Subsequently, fluoxetine and dizocilpine were docked using a molecular mechanics/grid method (Luty et al., 1995), employing the Affinity program (MSI, San Diego, CA, USA). The main molecular mechanics program employed in Affinity is also Discover and the CVFF force field including a desolvation term (Stouten et al., 1993).

The region corresponding to the pore of the ion channel was defined as the binding site region. In order to make the docking procedure faster, the system was partitioned into "bulk" (represented by grids) and "movable" atoms. Bulk atoms were defined as atoms of the receptor that were not in the defined binding site. These atoms were held rigid during the course of the docking search and represented by a grid. The potential energies due to the rigid atoms were calculated only once. Movable atoms consisted of atoms in the binding site of the ion channel and ligand atoms (fluoxetine and dizocilpine) were simulated explicitly. These atoms could move freely except for binding site atoms close to bulk atoms, which were restrained. These restrained atoms constitute a buffer which separated the freely movable atoms from bulk atoms.

Initially, fluoxetine and dizocilpine were placed arbitrarily in the AChR ion channel. This complex was then energy minimized to remove bad contacts in the initial structure and to obtain a reasonable starting point for subsequent searching. Next, the software moved the ligand by random combination of translation, rotation, and torsional changes. The random move of a ligand samples both the orientational and conformational spaces of the ligand with respect to the receptor. It is the first step to roughly docking the ligand and has the advantage of climbing any energy barrier on the potential energy surface. Affinity subsequently checked the energy of the resulting randomly moved structure. If it was within a specified energy tolerance parameter of the previous minimized structure, it was considered to have passed the first step and the structure was then subjected to energy minimization, the second step for fine-tuning the docking process. The final minimized structure was accepted or rejected based on the energy criterion and its similarity to structures found before. The energy criterion can be either Metropolis or energy range, and we used both in different runs. With the Metropolis criterion, structures whose energy was lower than that of the last accepted structure or whose Boltzmann factor (computed using specified Monte Carlo temperature) was greater than a random number between 0 and 1, were accepted. If energy range was used, structures with energies within the specified energy range of the lowest energy found so far were accepted. The Metropolis criterion is best suited for finding a very small number of docked structures with very low energies, while the energy range criterion is designed for finding a higher number of diverse structures. In checking structure similarity, the root mean square (RMS) distances between the current structure and structures found so far were computed for ligand atoms. In contrast to RMS deviation, in RMS distance the ligand molecule is not translated or rotated (i.e., no superimposition is done) because ligand/receptor structures with the ligand being translated or rotated are treated as different docked structures.

The parameters used in the docking procedures were a grid spacing of 0.66 Å, and a restrain buffer size of 0.5 Å. The energy range was set to 10 kcal mol^{-1}, that is, the program was asked to accept structures within 10 kcal mol^{-1} of the lowest energy structure found so far. We searched for a maximum of 10 different structures using the energy range method, and for all found after five days of simulation using Metropolis.

To estimate the energy of association for the fluoxetine and dizocilpine conformers, two different types of methods were used. The first calculation is a molecular mechanics based energy difference using Discover and the VCFF force field. In this method, free energies of binding for each conformer are calculated as the difference between the energy of the minimized ligand-receptor complex and the energies of the minimized ligand and receptor alone. This method of binding energy estimation is the one employed during the searching of the best conformers. The regression based score function method was used for comparison, but not for selecting the best conformations during the docking procedures. This method was developed by Böhm (Böhm, 1992, 1994), where an empirical scoring function for his *de novo* ligand design program, LUDI, predicts the binding free energy, ΔG. More specifically, ΔG is partitioned into six scoring terms: (1) overall rotational and translational entropy of the ligand, (2) hydrogen bonded interactions, (3) ionic interactions, (4) lipophilic interactions, (5) binding energy for freezing the rotable bonds, and (6) interaction between aromatic rings. LUDI score values for each analyzed ligand are related to K_i values in the form: score = 100 log K_i. LUDI scores can match or not the results obtained by the molecular mechanics approach when applied to all analyzed conformations.

3. Results

3.1. Inhibition of (±)-epibatidine-mediated Ca^{2+} influx in TE671 cells by SSRIs and dizocilpine

Increased concentrations of (±)-epibatidine activate the human embryonic muscle AChR (i.e., hα1β1γδ) with potency $EC_{50} = 0.26 \pm 0.04$ μM ($n_H = 1.23 \pm 0.06$; see Fig. 2), consistent with previous determinations (Michelmore et al., 2002; Arias et al., 2009). (±)-Epibatidine-induced hα1β1γδ AChR activation is blocked by pre-incubation (5 min) with fluoxetine or paroxetine with IC_{50} values (~2–5 μM) lower that that for dizocilpine (~21 μM) (Table 1). Interestingly, longer pre-incubation periods increased the potency of fluoxetine by ~10-fold (Table 1). The same effect was observed either at 4 or 24 h pre-incubation. The observed n_H values (Table 1) suggest that fluoxetine inhibits the ion channel in a non-cooperative manner.

3.2. Radioligand competition binding experiments using AChRs in different conformational states

Since the binding sites for PCP/TCP (Arias et al., 2002, 2003, 2006b; Sanghvi et al., 2008; Hamouda et al., 2008; Eaton et al., 2000) and dizocilpine (Arias et al., 2001) have been previously characterized in muscle-type AChRs, we want to determine the location of the SSRI binding site relative to these loci. In this regard, we first determined the influence of fluoxetine and paroxetine on [^{3}H]TCP

Author's personal copy

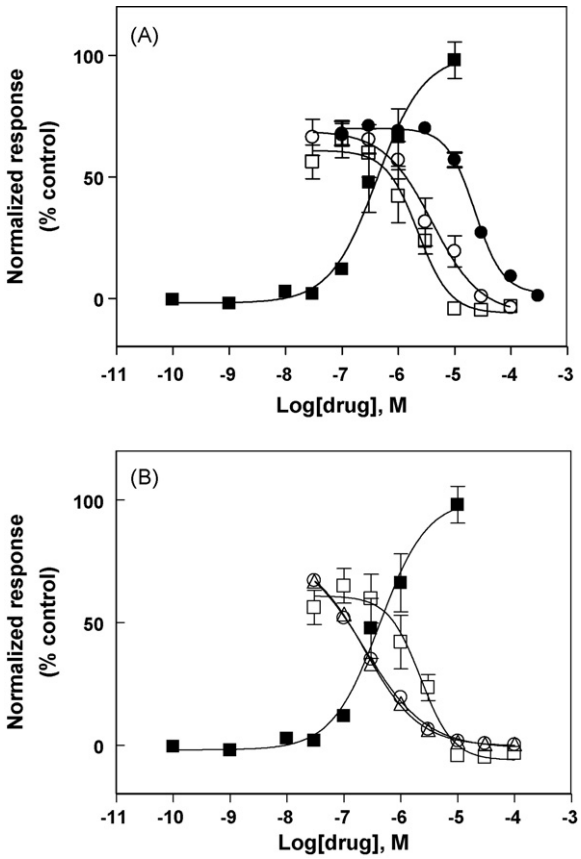

Fig. 2. Effect of SSRIs on (±)-epibatidine-induced Ca^{2+} influx in TE671-human α1β1γδ cells. Increased concentrations of (±)-epibatidine (■) activate the hα1β1γδ AChR with potency EC_{50} = 0.26 ± 0.04 μM (n_H = 1.23 ± 0.06). (A) Subsequently, cells were pre-treated (5 min) with several concentrations of fluoxetine (□) paroxetine (○) and dizocilpine (●). (B) Pre-treatment time for fluoxetine was increased from 5 min (□) to 240 min (○) or 1440 min (△), respectively. Thereafter, 1 μM (±)-epibatidine was added. Response was normalized to the maximal (±)-epibatidine response which was set as 100%. The plots are representative of 27 (■), four (●), and six (□, ○) determinations in (A), and three (○, △) determinations in (B), respectively. Error bars are S.D. The calculated IC_{50} and n_H values are summarized in Table 1.

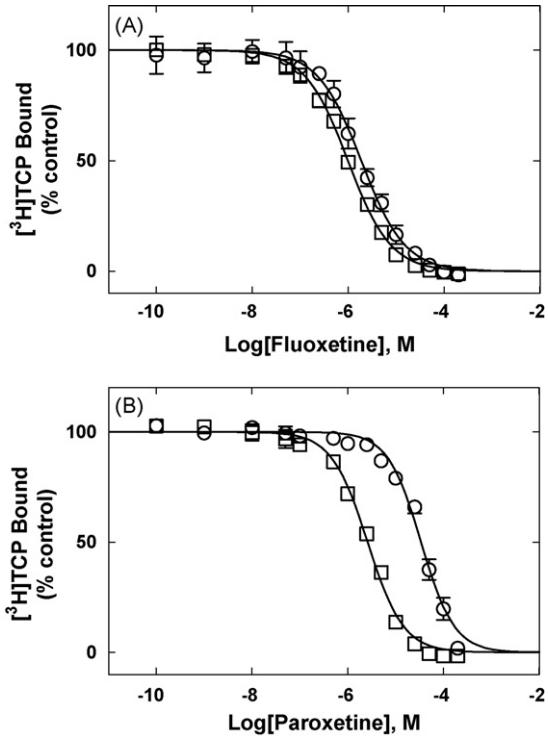

Fig. 3. Inhibition of [^{3}H]TCP binding to *Torpedo* AChRs in different conformational states elicited by (A) fluoxetine and (B) paroxetine. AChR-rich membranes (0.3 μM) were equilibrated (2 h) with 6.5 nM [^{3}H]TCP in the presence of 1 mM CCh (□) (desensitized/CCh-bound state), or with 9.2 nM [^{3}H]TCP in the presence of 1 μM α-BTx (○) (resting/α-BTx-bound state), and increasing concentrations of the SSRI under study (i.e., 1 nM–200 μM). Nonspecific binding was determined in the presence of 50 (□) or 100 μM PCP (○), respectively. Each plot is the combination of 2–5 separated experiments, each one performed in triplicate. From these plots the IC_{50} and n_H values were obtained by nonlinear least-squares fit according to Eq. (1). Subsequently, the K_i values were calculated using Eq. (2). The calculated K_i and n_H values are summarized in Table 2.

binding to the *Torpedo* AChR in different conformational states (Fig. 3). The results indicate that SSRIs bind to the [^{3}H]TCP site with ~2–13 times higher affinity in the desensitized/CCh-bound AChR than that in the resting/α-BTx-bound AChR (Table 2). Fluoxetine also inhibits the specific binding of [^{3}H]dizocilpine to the desensitized AChR (Fig. 4) with K_i = 1.9 μM (Table 2). Since [^{3}H]dizocilpine binds to the resting AChR with very low affinity (K_d ~ 140 μM; Arias et al., 2001), we did not performed the experiments in the resting state. The fact that the calculated n_H values for fluoxetine and paroxetine are close to unity (Table 2) indicates that SSRIs inhibit [^{3}H]TCP and [^{3}H]dizocilpine binding in a non-cooperative manner, suggesting that SSRIs interact with a single binding site.

3.3. Schild-plots for dizocilpine-induced inhibition of [^{3}H]TCP binding

We determined whether dizocilpine inhibits [^{3}H]TCP binding to the desensitized/CCh-bound AChR in a steric or allosteric manner by Schild-type analyses (Schild, 1949). Fig. 5A shows the dizocilpine-induced inhibition of [^{3}H]TCP binding at different initial concentrations of unlabeled PCP. At increased initial PCP concentrations, the plots were shifted to the right, indicating that higher dizocilpine amounts are required to inhibit the binding of [^{3}H]TCP at increased concentrations of unlabeled PCP (see Fig. 5A). By means of a modified Schild-type plot (Fig. 5B) (see Arias et al., 2002), we found a linear relationship between the initial concentration of PCP and the extent of radioligand inhibition with a goodness of fit value (r^2) of 0.89 (Fig. 5B). This suggests that dizocilpine inhibits [^{3}H]TCP binding to the desensitized/CCh-bound AChR by

Table 1
Inhibitory potency of SSRIs and dizocilpine on human embryonic muscle AChRs obtained by Ca^{2+} influx measurements.

NCA	Pre-incubation (min)	IC_{50}[a] (μM)	n_H[b]	Number of experiments (n)
Fluoxetine	5	1.8 ± 0.6	1.24 ± 0.08	6
	240	0.22 ± 0.01	0.85 ± 0.06	3
	1440	0.17 ± 0.08	0.89 ± 0.05	3
Paroxetine	5	4.8 ± 0.6	1.32 ± 0.31	6
Dizocilpine	5	21 ± 2	1.48 ± 0.20	4

[a] Required concentration of the NCA to produce 50% inhibition of agonist-activated AChRs (Fig. 2).
[b] Hill coefficient.

Author's personal copy

Table 2
Binding affinity of SSRIs to *Torpedo* AChRs in different conformational states.

Radioligand	SSRI	Desensitized/CCh-bound state		Resting/α-BTx-bound state	
		K_i (μM)[a]	n_H[b]	K_i (μM)[a]	n_H[b]
[^{3}H]TCP	Fluoxetine	0.96 ± 0.04	0.98 ± 0.03	1.9 ± 0.2	0.96 ± 0.09
	Paroxetine	2.5 ± 0.1	1.15 ± 0.05	34 ± 2	1.25 ± 0.09
[^{3}H]Dizocilpine	Fluoxetine	1.9 ± 0.2	0.84 ± 0.05	ND	ND

ND, not determined.
[a] Values were calculated from Fig. 3 ([^{3}H]TCP experiments) and Fig. 4 ([^{3}H]dizocilpine experiments), respectively, using Eq. (2).
[b] Hill coefficients.

a steric mechanism. Thus, we may infer that the dizocilpine locus overlaps the PCP binding site within the desensitized *Torpedo* AChR ion channel.

3.4. Modulation of [^{3}H]cytisine binding to Torpedo AChR by SSRIs

In order to determine the mechanisms of inhibition elicited by SSRIs, we studied the effect of fluoxetine and paroxetine on the binding of the agonist [^{3}H]cytisine to AChRs in distinct conformational states. Both fluoxetine (Fig. 6A) and paroxetine (Fig. 6B) enhance [^{3}H]cytisine binding to *Torpedo* AChRs in the resting but activatable state (in the absence of proadifen, a desensitizing local anesthetic). A potential explanation for this pharmacological effect is based on the fact that cytisine binds with ~4-fold higher affinity to the desensitized than that to the resting AChR (see Fig. 6C; Table 3). Another detail to take into consideration is that the AChR membrane suspension contains an excess of agonist binding sites (0.6 μM) compared with the initial concentration of [^{3}H]cytisine (7.7 nM). Since the cytisine K_i in the resting state is 1.6 μM (see Fig. 6C; Table 3), only a small fraction of AChRs will be initially labeled with [^{3}H]cytisine. Using Eq. (1), and considering $n_H = 1$ (see Table 3), a fractional occupancy (θ) of ~0.005% for [^{3}H]cytisine bound to the resting AChR was calculated. Thus, if the AChR is shifted to its high-affinity desensitized state, an increase in the fraction of AChR-bound [^{3}H]cytisine molecules can be expected. In this regard, using Eq. (1), and considering that the cytisine K_i in the desensitized state is 0.45 μM (see Table 3), a fractional occupancy of ~0.017% for [^{3}H]cytisine bound to the desensitized AChR was obtained. This is an increase of ~3-fold in fractional occupancy. Coincident with this calculation, our binding results indicate an increase of ~2-fold (see Fig. 6A and B). The explanation of these results is that when SSRIs bind to the ion channel, the AChR becomes desensitized, the affinity of [^{3}H]cytisine is increased and subsequently, a larger fraction of AChR-bound [^{3}H]cytisine is observed. In order to quantify this enhanced binding, the drug concentration to produce 50% increase of [^{3}H]cytisine binding was calculated (i.e., apparent EC_{50}s in Table 3). These values indicate that fluoxetine and paroxetine enhance [^{3}H]cytisine binding, probably by inducing AChR desensitization, with the same potency.

Fig. 6 also shows that SSRIs do not further enhance [^{3}H]cytisine binding to the already desensitized AChR (in the presence of 200 μM proadifen). This indicates that SSRIs do not induce any additional conformational change in the already desensitized AChR (i.e., maximal [^{3}H]cytisine binding). Moreover, SSRIs start inhibiting [^{3}H]cytisine binding at concentrations higher than 100 μM when the AChR is already desensitized. The apparent IC_{50} values for fluoxetine and paroxetine are in the ~2 mM concentration range (see Table 3), indicating that SSRIs bind to the agonist binding sites with extremely low affinity. Previous results are consistent with this observation (Fryer and Lukas, 1999), supporting the idea

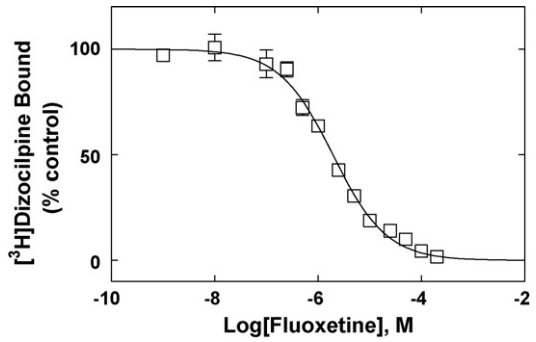

Fig. 4. Fluoxetine-induced inhibition of [^{3}H]dizocilpine binding to *Torpedo* AChRs in the desensitized state. AChR-rich membranes (0.3 μM) were equilibrated (2 h) with 20 nM [^{3}H]dizocilpine in the presence of 1 mM CCh (desensitized/CCh-bound state), and increasing concentrations of fluoxetine (i.e., 1 nM–200 μM). Nonspecific binding was determined in the presence of 400 μM dizocilpine. The plot is the combination of two separated experiments, each one performed in triplicate. From this plot the IC_{50} and n_H values were obtained by nonlinear least-squares fit according to Eq. (1). Subsequently, the K_i value was calculated using Eq. (2). The calculated K_i and n_H values are summarized in Table 2.

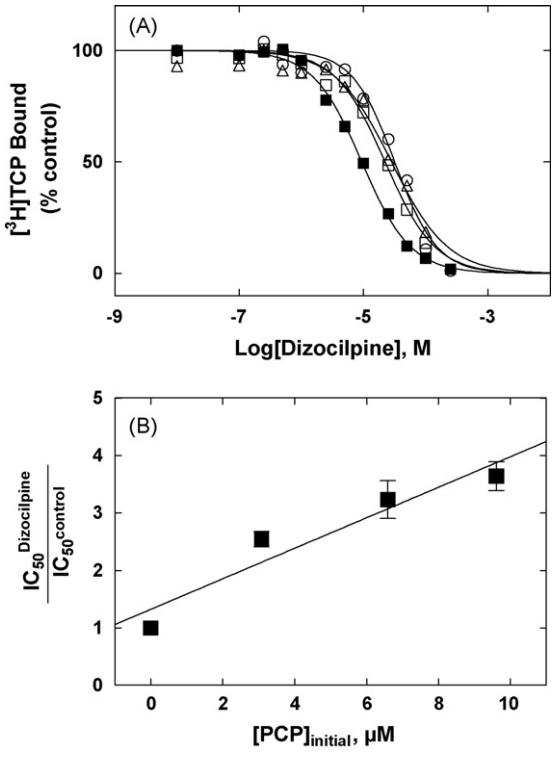

Fig. 5. Schild-plot for dizocilpine-induced inhibition of [^{3}H]TCP binding to the *Torpedo* AChR in the desensitized state. (A) AChR-rich membranes (0.3 μM nAChR) were equilibrated with [^{3}H]TCP, in the presence of 1 mM CCh (desensitized state), at initial PCP concentrations of 0 (control; (■), 3.1 (□), 6.6 (△), and 9.6 μM (○) respectively. The apparent IC_{50} values were calculated by nonlinear least-squares fit according to Eq. (1). Shown is the average of experiments performed in triplicate. (B) Modified Schild-plot for dizocilpine-induced inhibition of [^{3}H]TCP binding. The plot shows a linear relationship with a r^2 value of 0.89, suggesting that dizocilpine inhibits [^{3}H]TCP binding by a steric mechanism. Shown is the mean ± SD from experiments performed in triplicate.

Author's personal copy

Table 3
Modulation of agonist binding to *Torpedo* AChRs in different conformational states.

Radioligand	Ligand	Resting but activatable state		Desensitized/proadifen-bound state	
		Apparent EC_{50} [a] (μM)	Apparent n_H [d]	Apparent IC_{50} [b] (mM)	Apparent n_H [d]
[^{3}H]Cytisine	Fluoxetine	2.8 ± 0.8	0.97 ± 0.24	1.6 ± 0.9	0.74 ± 0.19
	Paroxetine	2.6 ± 0.9	0.98 ± 0.32	2.3 ± 1.5	0.38 ± 0.11
		K_i (μM) [c]	n_H [d]	K_i (μM) [c]	n_H [d]
[^{3}H]Nicotine	Cytisine	1.6 ± 0.1	1.08 ± 0.10	0.45 ± 0.06	1.14 ± 0.15

[a] SSRI concentration required to enhance 50% [^{3}H]cytisine binding was obtained using AChRs in the resting but activatable state (in the absence of any ligand) (Fig. 6A and B).
[b] SSRI concentration required to inhibit 50% [^{3}H]cytisine binding was obtained using AChRs in the desensitized state (in the presence of 200 μM proadifen) (Fig. 6A and B).
[c] Inhibiton constants for cytisine were obtained from Fig. 6C, using Eq. (2).
[d] Hill coefficient.

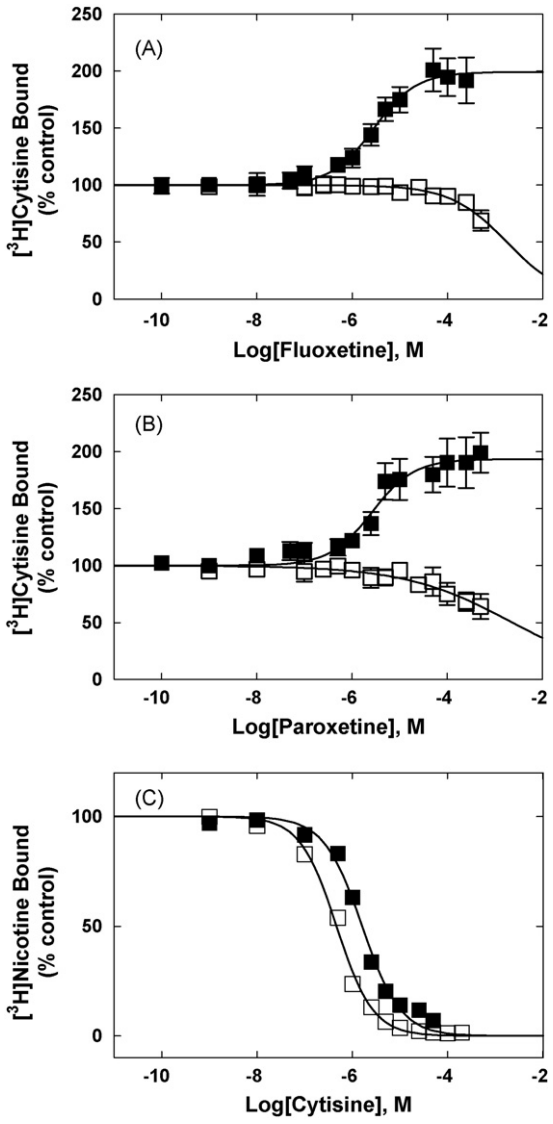

Fig. 6. Modulation of [^{3}H]cytisine binding to *Torpedo* AChRs elicited by fluoxetine (A) and paroxetine (B) in the resting but activatable and desensitized states, respectively. (C) Cytisine-induced inhibition of [^{3}H]nicotine binding to *Torpedo* AChRs in the resting but activatable and desensitized states, respectively. AChR native membranes (0.3 μM nAChR) were equilibrated (30 min) with 7.7 nM [^{3}H]cytisine (A and B) or with 6.9 nM [^{3}H]nicotine (C), in the absence (resting but activatable state) (■) or in the presence of 200 μM proadifen (desensitized/proadifen-bound state) (□), and increasing concentrations of the ligand under study. The apparent IC_{50} (or apparent EC_{50}) and n_H values were obtained according to Eq. (1), and summarized in Table 4. Shown is the mean ± SD from 2–3 experiments, each one performed in triplicate.

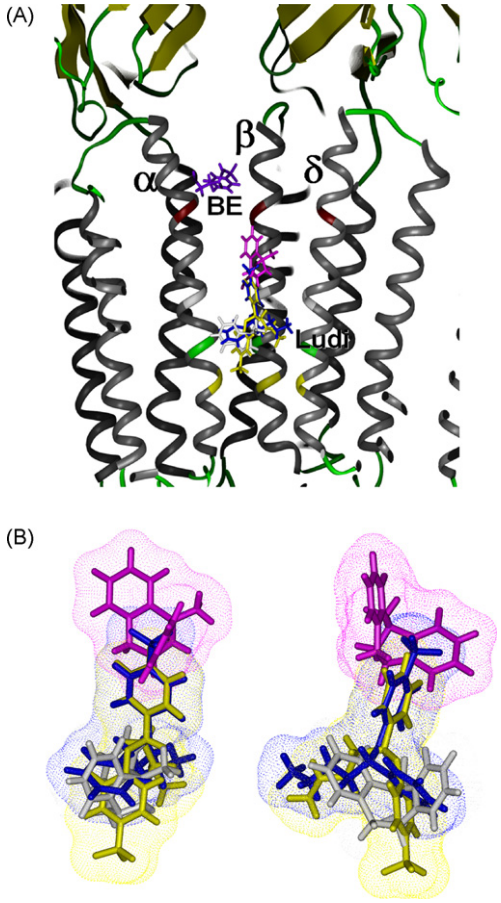

Fig. 7. (A) Schematic representation of the cross-section of the *Torpedo* AChR ion channel showing the docked fluoxetine and dizocilpine in the neutral and protonated forms. The ribbons represent the transmembrane helices from the α1, β1, and δ subunits, parallel to the membrane plane. In the center, three ribbons corresponding to the M2 helices have differentially colored the main amino acid rings including, the serine (position 6′; yellow), leucine (position 9′; green), valine (position 13′; grey), and outer (position 20′; red) rings, respectively. In stick representation, the docked molecules are colored in yellow (neutral fluoxetine), purple ("BE protonated fluoxetine"), blue ("Ludi protonated fluoxetine"), white (neutral dizocilpine), and magenta (protonated dizocilpine), respectively. (B) Detailed view of the overlapping docking between both molecular states of fluoxetine and dizocilpine. Protonated fluoxetine corresponds to "Ludi protonated fluoxetine". The two images are zoomed and rotated views of the binding site locations modeled in (A), showing only four of the docked molecules. In stick representation and surrounded by their corresponding accessible surfaces, the docked molecules are colored as in (A). Fluoxetine overlaps both neutral (completely) and protonated (partially) dizocilpine (For interpretation of the references to color in this figure legend, the reader is referred to the web version of the article).

Author's personal copy

that the pharmacological action of these antidepressants is not mediated by a competitive but by a noncompetitive inhibition of AChRs.

3.5. Molecular docking of fluoxetine and dizocilpine in the Torpedo AChR ion channel

Molecular docking simulations of fluoxetine and dizocilpine in the *Torpedo* AChR ion channel showed that these two molecules share the same binding site in their neutral state (Fig. 7). Both fluoxetine (Fig. 8A and B) and dizocilpine (Fig. 9A and B) in the neutral state interact with the leucine (position 9′) and valine (position 13′) rings of the AChR ion channel. These neutral drugs also have the same binding affinities according to the two estimation methods (Table 4). Nevertheless, fluoxetine and dizocilpine dock in slightly different luminal positions when they are protonated. These protonated drugs have the highest but similar affinity values (Table 4). According to the affinity estimated using binding energies, the best conformer of protonated fluoxetine (named hereon "BE protonated fluoxetine") docks close to the extracellular ion channel mouth, interacting with residues at or surrounding the outer ring (position 20′) by electrostatic interactions (see Fig. 8C and D). However, according to LUDI scores, the best conformer of protonated fluoxetine ("Ludi protonated fluoxetine") docks in the same loci as neutral fluoxetine and dizocilpine (Figs. 7 and 8E and F). Protonated dizocilpine bridges these two binding sites by interacting with a domain spanning from the valine (position 13′) to the outer (position 20′) ring (see Fig. 9C and D). Considering that protonated dizocilpine is located in an intermediate site along the ion channel, it partially overlaps the docking site for neutral and "BE protonated fluoxetine" (Fig. 7). This figure also shows that in either molecular state, dizocilpine interferes with the binding of neutral fluoxetine.

Interaction energies including, electrostatic or Coulombic and van der Waals energies, between the ligand and individual receptor residues within a cut-off distance of 4 Å were calculated (Table 5). The analysis of interaction energies shows that neutral and protonated fluoxetine differ markedly with respect to the main force types involved in their docking (see Table 5). The binding energies of neutral fluoxetine, "Ludi protonated fluoxetine", and neutral dizocilpine are markedly hydrophobic (98%, 99%, and 97% of the total energy, respectively). On the other hand, the electrostatic interactions rise to 48% for "BE protonated fluoxetine", and with less strength protonated dizocilpine rises from 3% to 10%.

The first four ranked ion channel residues for the best docked conformers of fluoxetine and dizocilpine were determined according to their receptor residue binding energies (Table 6). Neutral fluoxetine interacts mainly with residues γ-Ile263 and α1-Val255 at the valine ring (position 13′), and with α1-Leu251 at the leucine ring (position 9′) by hydrophobic contacts (Fig. 8A and B; Table 6). Neutral fluoxetine has also a small but unfavorable electrostatic interaction with δ-Val269 (position 13′) that is compensated by a higher van der Waals component (see Table 6). Overall, the most important interactive forces with the four main residues are hydrophobic as shown in Table 5. Neutral dizocilpine also has hydrophobic interactions with the same rings, but with higher influence of the residues γ-Leu259, α1-Leu251, and β1-Leu257 at the leucine ring (Fig. 9A and B). Likewise, the main interacting forces for neutral fluoxetine remain hydrophobic, but with a slight increase of Coulombic energies (from 3% to 13%; compare Tables 5 and 6). The forces involved in the interaction of "BE protonated fluoxetine" with the main four ion channel residues are highly electrostatics (52%, Table 6). One of them is a hydrogen bond between the backbone oxygen of γ-Gln270 and a hydrogen from the ammonium moiety of fluoxetine. In addition, "BE protonated fluoxetine" makes electrostatic contacts predominantly with acidic residues including, α1-Glu262 and β1-Asp269 at the outer ring (position 20′), and γ-Glu274 located outside the ion channel mouth (as usually defined) at position 24′. "BE protonated fluoxetine" also interacts with the backbone oxygen atom from γ-Lys271 (position 21′), while the side chain of this residue does not face the ion channel lumen. "Ludi protonated fluoxetine" interacts with almost the same rings as those involved with neutral fluoxetine and neutral dizocilpine. However, in this case the main forces are electrostatics (56%; Table 6), contrary to the highly hydrophobic interaction (99%; Table 5) measured for the 18 residues within the 4 Å limit. More specifically, the ammonium moiety of "Ludi protonated fluoxetine" forms a hydrogen bond with the backbone oxygen from β1-Leu257 (position 9′) (Fig. 8E), and van der Waals and electrostatic interactions between its ammonium and methyl moieties and the δ-Leu265 side chain (position 9′). In addition, there are electrostatic interactions between the ammonium moiety with the backbone oxygen of β1-Ala258 (position 10′), and hydrophobic interactions between its trifluoromethyl and phenyl moieties with the γ-Ile263 side chain (position 13′) (see Fig. 8E and F; Table 6). This sort of interaction, with a strong local Coulombic force in an otherwise hydrophobic environment, might be the reason of the different results obtained by the two methods employed for drug affinity estimations. Thus, in the docking of "BE protonated fluoxetine", where the drug binds to a wide section of the ion channel with less direct contacts with luminal residues, the interaction that prevails is electrostatic. On the other hand, in the docking of "Ludi protonated fluoxetine", where the drug binds to a narrow part of the ion channel with an extensive surface contact, van der Waals forces are overall more important, but nevertheless, the binding is reinforced by a localized electrostatic force represented by a hydrogen bond.

Albeit in a different deeper position along the ion channel, protonated dizocilpine is docked between the valine and outer rings, mainly by a hydrogen bond between the backbone oxygen of δ-Val269 (position 13′) and a hydrogen from its ammonium moiety (Fig. 9C and D). Although protonated dizocilpine has an unfavorable electrostatic interaction with γ-Leu267 (position 17′), it is well compensated with a strong hydrophobic contact (see Table 6) mediated by the contacts between the γ-Leu267 side chain and the aromatic rings of protonated dizocilpine. Protonated dizocilpine also makes contacts with the backbone atoms of δ-Phe270 at position 14′, whose side chain is buried at the helical interface between the δ and α1 subunits (Table 6; Fig. 9C and D). At position 20′, the interaction with γ-Gln270 is approximately half electrostatic and half hydrophobic (Table 6). These involve electrostatic interactions between the amide oxygen of γ-Gln270 side chain and the dizocilpine ammonium moiety, and van der Waals interactions mediated by one of the phenyl groups of dizocilpine and the γ-Gln270 side chain. The most important forces involved between protonated dizocilpine and the main four residues are mostly electrostatics, comprising 57% of the total energy (Table 6), similar to those for both Ludi and BE conformers of protonated fluoxetine.

4. Discussion

SSRIs inhibit several AChRs in a noncompetitive manner and this pharmacological activity might be relevant for the therapeutic treatment of mental depression and slow-channel congenital myasthenic syndromes (see Section 1. for details). In this regard, the inhibitory mechanisms and the binding site location for fluoxetine and paroxetine on AChRs in different conformational states were determined using structural and functional approaches.

Regarding the functional aspects of SSRIs, the Ca^{2+} influx results indicate that fluoxetine and paroxetine inhibit the AChR with potencies higher than that for dizocilpine (see Table 1). The

Author's personal copy

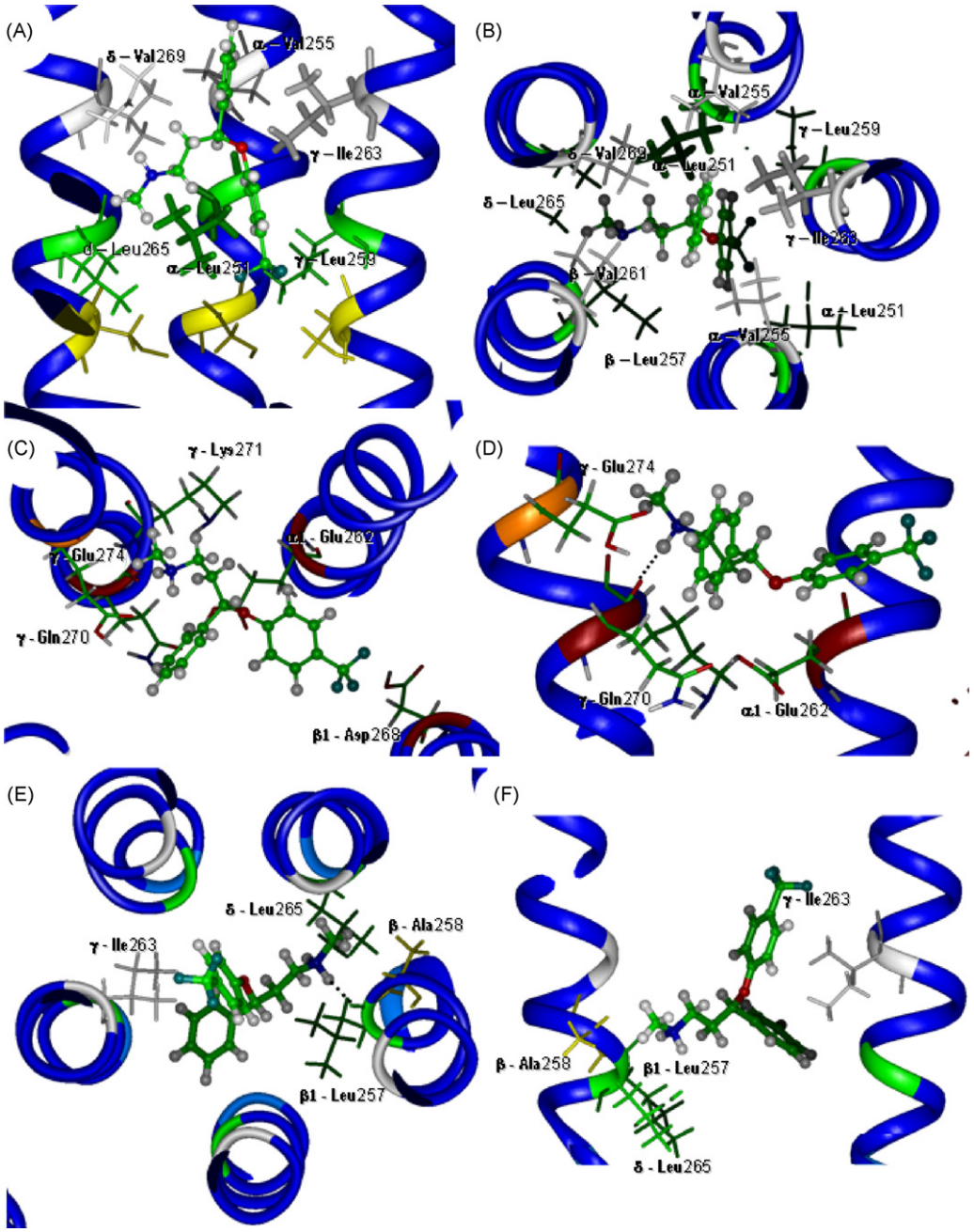

Fig. 8. Fluoxetine docked in the *Torpedo* AChR ion channel. Fluoxetine is depicted in ball and stick. AChR residues forming the amino acid rings are shown as stick representation, and their van der Waals surfaces are colored in yellow (serine ring; position 6′), green (leucine ring; position 9′), grey (valine ring; position 13′), red (outer ring; position 20′), and orange (position 24′), respectively. Lateral (A) and extracellular (B) views of the *Torpedo* AChR ion channel interacting with neutral fluoxetine. The main residues, γ-Ile263 (position 13′) and α1-Leu251 (position 9′), interacting with neutral fluoxetine are represented in thick sticks. Extracellular (C) and lateral (D) views of the *Torpedo* AChR ion channel interacting with "BE protonated fluoxetine". Acidic residues including, α1-Glu262 at the outer ring (position 20′) and γ-Glu274 (position 24′) are shown along with the backbone atoms of γ-Lys271 (position 21′) interacting with "BE protonated fluoxetine" by Coulombic forces. The hydrogen bond between protonated fluoxetine and γ-Gln270 (position 20′) is depicted with a dotted line. Extracellular (E) and lateral (F) views of the *Torpedo* AChR ion channel interacting with "Ludi protonated fluoxetine". The hydrogen bond between "Ludi protonated fluoxetine" and β1-Leu257 (position 9′) is depicted with a dotted line. For further details see Table 6 (For interpretation of the references to color in this figure legend, the reader is referred to the web version of the article).

observed values for fluoxetine and paroxetine were the same as previously determined (Fryer and Lukas, 1999; García-Colunga and Miledi, 1999). The observed IC_{50} value for dizocilpine is closer to that found for β2- than that for β4-containing AChRs (Yamakura et al., 2000). Interestingly, the potency of fluoxetine was increased 10-fold with longer pre-incubation periods (see Table 1). An obvious explanation is that the AChR is desensitized in the prolonged presence of fluoxetine, and thus, the affinity and potency of fluoxetine is increased. However, we cannot rule out other pleotropic mechanisms such as modulation of AChR phosphorylation, lipid membrane, and Ca^{2+} homeostasis, especially considering that fluoxetine is membrane permeable.

After prolonged treatment of slow-channel congenital myasthenic syndrome patients with 80–120 mg fluoxetine per day, total plasma concentrations of ~8–11 μM were found for both fluoxetine and its active metabolite norfluoxetine (Harper et al., 2003). It is very clear from our Ca^{2+} influx results at prolonged pre-incubation times that the active concentration (~10%) of fluoxetine (~1 μM) can block muscle AChRs, producing its beneficial effect on these pathological cases.

Author's personal copy

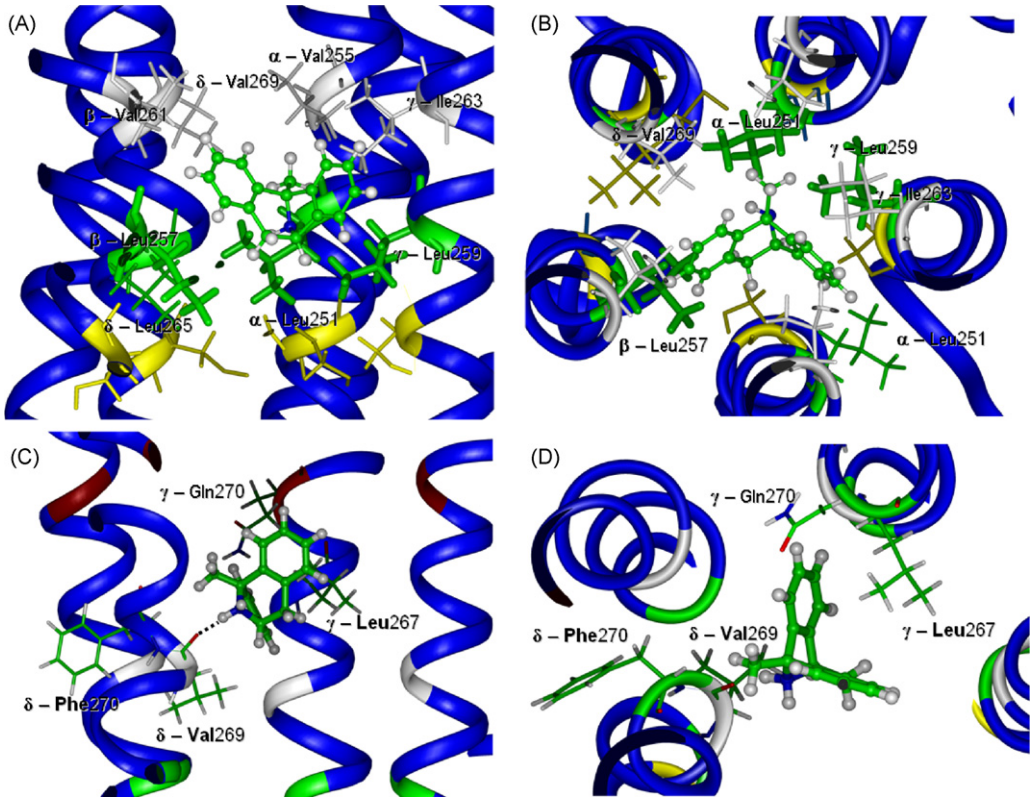

Fig. 9. Dizocilpine docked in the *Torpedo* AChR ion channel. Dizocilpine is depicted in ball and stick. AChR residues forming the amino acid rings are shown as stick representation, and their van der Waals surfaces are colored in yellow (serine ring; position 6′), green (leucine ring; position 9′), and grey (valine ring; position 13′), respectively. Lateral (A) and extracellular (B) views of the *Torpedo* AChR ion channel interacting with neutral dizocilpine. The main residues, γ-Leu259, α1-Leu251, and β1-Leu257 (position 9′), interacting with neutral dizocilpine are represented in thick sticks. Extracellular (C) and lateral (D) views of the *Torpedo* AChR ion channel interacting with protonated dizocilpine. The main residues, δ-Val269 (position 13′), δ-Phe270 (position 14′), γ-Leu267 (position 17′), and γ-Gln270 (position 20′), interacting with protonated dizocilpine are represented by sticks. The hydrogen bond between protonated dizocilpine and δ-Val269 (position 13′) is depicted with a dotted line. δ-Val269 and δ-Phe270 have mainly electrostatic interactions with protonated dizocilpine, γ-Leu267 has mainly hydrophobic contacts, while γ-Gln270 has electrostatic and hydrophobic interactions equally important. For further details see Table 6 (For interpretation of the references to color in this figure legend, the reader is referred to the web version of the article).

Table 4
Ligand affinity estimations based on docking simulations.

Ligand	Molecular state	Binding energy[a] (kcal mol^{-1})	LUDI [b]	
			Score	Predicted K_i [c] (μM)
Fluoxetine	Neutral	−61.6	407	85
	"BE protonated"	−120.9	–	–
	"Ludi protonated"	−105.3	452	30
Dizocilpine	Neutral	−48.8	408	83
	Protonated	−107.0	440	40

[a] Values were obtained using a molecular mechanics approximation (see details in Section 2).
[b] Values were obtained using the LUDI score method (see details in Section 2).
[c] Values were obtained using the relationship: LUDI score = 100 log K_i.

Table 5
Calculated binding energies of fluoxetine and dizocilpine interacting with residues within 4 Å limit in the *Torpedo* AChR ion channel.

Ligand	Molecular form	Number of residues involved	Binding energy[a] (kcal mol^{-1})		
			Coulombic	van der Waals	Total
Fluoxetine	Neutral	19	−0.5 (2%)	−23.4 (98%)	−23.9
	"BE Protonated"	9	−13.2 (48%)	−14.3 (52%)	−27.5
	"Ludi Protonated"	18	−0.2 (1%)	−21.0 (99%)	−21.2
Dizocilpine	Neutral	15	−0.7 (3%)	−19.6 (97%)	−20.3
	Protonated	14	−2.0 (10%)	−18.1 (90%)	−20.1

Between parentheses are the percentages of the different energy type respect to the total energy.
[a] Binding energy for the different types of interactions. Values were obtained using a molecular mechanics approximation (see details in Methods).

Author's personal copy

Table 6
Calculated binding energies of fluoxetine and dizocilpine interacting with the main residues within the *Torpedo* AChR ion channel.

Ligand	Molecular form	Position	Residue	Energy (kcal mol^{-1})[a]		
				Coulombic [b]	van der Waals	Total
Fluoxetine	Neutral	9′	α1-Leu251	−0.02	−2.5	−2.5
		13′	γ-Ile263	−0.1	−2.4	−2.5
			α1-Val255	−0.2	−2.0	−2.2
			δ-Val269	0.1	−1.9	−1.8
		Energy percentages		2%	98%	
	"BE protonated"	20′	γ-Gln270	−6.4 [c]	−2.1	−8.5
			α1-Glu262	−0.1	−3.4	−3.5
		21′	γ-Lys271	−2.2	−1.7	−4.0
		24′	γ-Glu274	−1.7	−2.3	−4.0
		Energy percentages		52%	48%	
	"Ludi protonated"	9′	β1-Leu257	−4.3 [c]	−0.2	−4.5
			δ-Leu265	−1.2	−1.2	−2.3
		10′	β1-Ala258	−1.5	−0.7	−2.2
		13′	γ-Ile263	0.7	−2.9	−2.3
		Energy percentages		56%	44%	
Dizocilpine	Neutral	9′	γ-Leu259	−0.4	−2.6	−3.0
			α1-Leu251	−0.4	−1.9	−2.3
			β1-Leu257	−0.3	−1.9	−2.3
		13′	γ-Ile263	−0.03	−1.6	−1.6
		Energy percentages		13%	87%	
	Protonated	13′	δ-Val269	−5.9 [c]	-0.5	−6.4
		17′	γ-Leu267	0.5	−3.3	−2.8
		14′	δ-Phe270	−1.3	−0.7	−2.0
		20′	γ-Gln270	−0.8	−1.0	−1.8
		Energy percentages		57%	43%	

[a] Values were obtained using a molecular mechanics approximation (see details in Section 2).
[b] Negative values indicate attraction between molecules, whereas positive values indicate repulsive interaction.
[c] Includes the energy derived from one hydrogen bond.

Previous electrophysiological studies indicated that SSRIs induce desensitization in different AChRs (García-Colunga et al., 1997; López-Valdés and García-Colunga, 2001). The observed enhanced [^{3}H]cytisine binding to the resting but activatable *Torpedo* AChR (see Fig. 6A and B) and the increased inhibitory potency after prolonged pre-incubation periods (Table 1) by SSRIs support these previous results. In this regard, SSRIs may modulate the function of AChRs by a combination of ion channel blocking and desensitization processes. The same combined inhibitory mechanisms were previously determined for tricyclic antidepressants and bupropion in different AChR subtypes (Gumilar et al., 2003; López-Valdés and García-Colunga, 2001; Arias et al., 2009; Gumilar and Bouzat, 2008). This evidence suggests that there is a basic mechanistic motif for structurally different antidepressants underlying the inhibition of distinct AChRs. AChR desensitization, as part of its inhibitory mechanism, might play an important role in the therapeutic activity of these compounds in depression and other neurological disorders (e.g., Mineur et al., 2009 and references therein; reviewed in Shytle et al., 2002; Arias, 2009).

The results from the [^{3}H]TCP competition binding experiments indicate that SSRIs bind with higher affinity to the desensitized *Torpedo* AChR compared to the resting AChR (see Table 2). The same trend was observed with the [^{3}H]dizocilpine competition experiment results (Table 2). Our results suggest that SSRIs interact with both PCP and dizocilpine binding sites in a steric fashion. However, the dizocilpine binding site has been considered to be structurally related to the quinacrine site (Arias et al., 2001), which is located at the non-annular lipid domain of the AChR (Arias, 1997), rather than at the PCP locus. There are at least two possible scenarios to explain this dichotomy. The first explanation is that quinacrine and PCP share the same binding site. This option has been supported by cysteine-substituted mutant experiments where the potential binding site for quinacrine coincides with that for PCP (Yu et al., 2003). The second explanation is that dizocilpine in fact overlaps the PCP binding site. The results indicating that dizocilpine displaces [^{3}H]TCP binding to the desensitized AChR with low K_i and with a n_H value close to unity (Arias et al., 2001) supports this possibility. Our Schild-analysis indicates that dizocilpine displaces [^{3}H]TCP binding by a steric mechanism (Fig. 5), suggesting overlapping sites. Subsequently, the binding site for SSRIs may overlap both the PCP and dizocilpine loci in the desensitized AChR ion channel.

The molecular modeling results support these conclusions (Table 6, Fig. 7). First, neutral fluoxetine (Fig. 8A and B) and "Ludi protonated fluoxetine" (Fig. 8E and F), as well as dizocilpine in the neutral state (Fig. 9A and B), bind to overlapping sites located between the leucine (position 9′) and valine (position 13′) rings. This location coincides with that determined for PCP in the desensitized *Torpedo* AChR ion channel (Arias et al., 2003, 2006b; Sanghvi et al., 2008; Hamouda et al., 2008). Second, protonated dizocilpine binds between the valine (position 13′) and outer (position 20′) rings, with the subsequent partial overlapping with neutral fluoxetine (Fig. 7B). The overlapping between the neutral fluoxetine site and the domain for dizocilpine in the neutral and protonated states (Fig. 7) is in agreement with the binding results (Table 2). On the other hand, "BE protonated fluoxetine" makes contacts predominantly with residues at or close to the extracellular mouth of the ion channel (Fig. 8C and D). This result is in agreement with the "electrical distance" of fluoxetine (∼0.20–0.25) estimated by voltage-clamp studies, indicating that the site of action of SSRIs in the activated α1β1γδ ion channel is located close to the extracellular mouth of the ion channel (García-Colunga et al., 1997; García-Colunga and Miledi, 1999).

The binding site location for "BE protonated fluoxetine" and protonated dizocilpine is similar to that considered for PCP in the resting *Torpedo* AChR (Arias et al., 2002, 2003, 2006b; Sanghvi et al., 2008). It was shown that the binding site for PCP in the resting state is very wide and that the only restriction for binding was the presence of a protonated amino group. A plausible model is that

Author's personal copy

the docking sites for the protonated fluoxetine and dizocilpine are pharmacologically important in the first stages of channel blocking by attracting the molecules to the ion channel mouth. This mechanism agrees well with the high percentages of protonated fluoxetine (~95%) and dizocilpine (~99%) at physiological pH, estimated by using their pK_a values (9.5 for dizocilpine and 8.7 for fluoxetine; Tetko et al., 2005). This model might be especially true for the *Torpedo* AChR ion channel, since it is the only AChR type with two extra acidic residues at position 24′ (i.e., β1 and γ subunits) that are lacking in the neuronal AChR subtypes.

Considering this binding site model, a dynamic mechanism of noncompetitive inhibition can be hypothesized: the protonated drug is first attracted by electrostatic interactions to the extracellular entrance of the ion channel, and upon ligand binding, the neutral form is stacked in a narrower and deeper section of the ion channel and stabilized by van der Waals contacts. How the ionic forms are deprotonated is not known. We only can speculate that in a large domain as the extracellular channel mouth, few water molecules can be accommodated around a small molecule and consequently it can still maintain certain degree of protonation in its locus, whereas the interaction with a hydrophobic and smaller environment deeper in the ion channel decreases the possibility of a larger molecule to be hydrated and consequently, it is unlikely that the bound state is actually in the protonated form. This model is supported by the dynamic analysis of water molecules along the ion channel, where the water mobility (Smith and Sansom, 1997) and the possibility of hydration (Beckstein and Sansom, 2004) are reduced in a narrow space within the ion channel lumen. Another plausible scheme is that the conformational changes produced during channel gating and opening and the initial ion flux can destabilize the established electrostatic interactions. This might be especially true for hydrogen bonds where the geometry of the interaction is important.

Acknowledgements

This research was supported by grants from the Science Foundation Arizona and Stardust Foundation and from the Office of Research and Sponsored Programs, Midwestern University (to H.R.A.), and by CONICET, Argentina (to M.O.). Pankaj Bhumireddy was supported by the Master of Science in Pharmaceutical Sciences Program, College of Pharmacy, Western University of Health Sciences, Pomona, CA, USA. The authors thank the National Institute on Drug Abuse (NIDA) for the gift of phencyclidine. We also thank to Jorgelina L. Arias Castillo and Paulina Iacoban for their technical assistance, and to Dr. Mark Olsen (Midwestern University) for his help with the English language.

References

Albuquerque EX, Pereira EFR, Alkondon A, Rogers SW. Mammalian nicotinic acetylcholine receptors: from structure to function. Physiol Rev 2009;89:73–120.
Aracava Y, Albuquerque EX. Meproadifen enhances activation and desensitization of the acetylcholine receptor-ionic channel complex (AChR): single channel studies. FEBS Lett 1984;174:267–74.
Arias HR. The high-affinity quinacrine binding site is located at a non-annular lipid domain of the nicotinic acetylcholine receptor. Biochim Biophys Acta 1997;1347:9–22.
Arias HR. Ligand-gated ion channel receptor superfamilies. In: Arias HR, editor. Biological and Biophysical Aspects Of Ligand-Gated Ion Channel Receptor Superfamilies. India: Research Signpost; 2006. p. 1–25, chapter 1.
Arias HR. Is the inhibition of nicotinic acetylcholine receptors by bupropion involved in its clinical actions? Int J Biochem Cell Biol 2009;41:2098–108.
Arias HR, McCardy EA, Blanton MP. Characterization of the dizocilpine binding site on the nicotinic acetylcholine receptor. Mol Pharmacol 2001;59:1051–60.
Arias HR, McCardy EA, Bayer EZ, Gallagher MJ, Blanton MP. Allosterically linked noncompetitive antagonist binding sites in the resting nicotinic acetylcholine receptor ion channel. Arch Biochem Biophys 2002;403:121–31.
Arias HR, Trudell JR, Bayer EZ, Hester B, McCardy EA, Blanton MP. Noncompetitive antagonist binding sites in the *Torpedo* nicotinic acetylcholine receptor ion channel. Structure-activity relationship studies using adamantane derivatives. Biochemistry 2003;42:7358–70.
Arias HR, Bhumireddy P, Bouzat C. Molecular mechanisms and binding site locations for noncompetitive antagonists of nicotinic acetylcholine receptors. Int J Biochem Cell Biol 2006a;38:1254–76.
Arias HR, Bhumireddy P, Spitzmaul G, Trudell JR, Bouzat C. Molecular mechanisms and binding site location for the noncompetitive antagonist crystal violet on nicotinic acetylcholine receptors. Biochemistry 2006b;45:2014–26.
Arias HR, Gumilar F, Rosenberg A, Targowska-Duda KM, Feuerbach D, Jozwiak K, et al. Interaction of bupropion with muscle-type nicotinic acetylcholine receptors in different conformational states. Biochemistry 2009;48:4506–18.
Beckstein O, Sansom M. The influence of geometry, surface character, and flexibility on the permeation of ions and water through biological pores. Phys Biol 2004;1:42–52.
Böhm HJ. The computer-program LUDI – a new method for the *de novo* design of enzyme-inhibitors. J Comput Aided Mol Des 1992;6:61–78.
Böhm HJ. The development of a simple empirical scoring function to estimate the binding constant for a protein ligand complex of known 3-dimensional structure. J Comput Aided Mol Des 1994;8:243–56.
Cheng Y, Prusoff WH. Relationship between the inhibition constant (K_i) and the concentration of inhibitor which causes 50 percent inhibition (IC_{50}) of an enzymatic reaction. Biochem Pharmacol 1973;22:3099–108.
Doucet J-P, Weber J. Empirical force field methods and molecular mechanics. In: Doucet J-P, Weber J, editors. Computer-Aided Molecular Design. San Diego: Academic Press; 1996. p. 124–70.
Eaton MJ, Labarca C, Eterović VA. M2 Mutations of the nicotinic acetylcholine receptor increase the potency of the noncompetitive inhibitor phencyclidine. J Neurosci Res 2000;61:44–51.
Fryer JD, Lukas RJ. Antidepressants noncompetitively inhibit nicotinic acetylcholine receptor function. J Neurochem 1999;72:1117–24.
García-Colunga J, Miledi R. Blockage of mouse muscle nicotinic receptors by serotonergic compounds. Exp Physiol 1999;84:847–64.
García-Colunga J, Awad JN, Miledi R. Blockage of muscle and neuronal nicotinic acetylcholine receptors by fluoxetine (Prozac). Proc Natl Acad Sci USA 1997;94:2041–2.
García-Colunga J, Vázquez-Gómez E, Miledi R. Combined actions of zinc and fluoxetine on nicotinic acetylcholine receptors. Pharmacogenomics J 2004;4:388–93.
Gumilar F, Bouzat C. Tricyclic antidepressant inhibit homomeric Cys-Loop receptors by acting at different conformational states. Eur J Pharmacol 2008;584:30–9.
Gumilar F, Arias HR, Spitzmaul G, Bouzat C. Molecular mechanism of inhibition of nicotinic acetylcholine receptors by tricyclic antidepressants. Neuropharmacology 2003;45:964–76.
Hamouda AK, Chiara DC, Blanton MP, Cohen JB. Probing the structure of the affinity-purified and lipid-reconstituted *Torpedo* nicotinic acetylcholine receptor. Biochemistry 2008;47:12787–94.
Harper CM. Congenital myasthenic syndromes. Semin Neurol 2004;24:111–23.
Harper CM, Fukodome T, Engel AG. Treatment of slow-channel congenital myasthenic syndrome with fluoxetine. Neurology 2003;60:1710–3.
Keserü G, Kolossváry I. Molecular Mechanics and Conformational Analysis in Drug Design. Oxford: Blackwell Science Ltd; 1999. pp. 1–168.
López-Valdés HE, García-Colunga J. Antagonism of nicotinic acetylcholine receptors by inhibitors of monoamine uptake. Mol Psychiatry 2001;6:511–9.
Luty BA, Wasserman ZR, Stouten PFW, Hodge CN, Zacharias M, Mccammon JA. A molecular mechanics grid method for evaluation of ligand- receptor interactions. J Comput Chem 1995;16:454–64.
Maggi L, Palma E, Miledi R, Eusebi F. Effects of fluoxetine on wild and mutant neuronal α7 nicotinic receptors. Mol Psychiatry 1998;3:350–5.
Michelmore S, Croskery K, Nozulak J, Hoyer D, Longato R, Weber A, et al. Study of the calcium dynamics of the human α4β2, α3β4 and α1β1γδ nicotinic acetylcholine receptors. Naunyn-Schmiedebergs Arch Pharmacol 2002;366:235–45.
Middleton RE, Cohen JB. Mapping of the acetylcholine binding site of the nicotinic acetylcholine receptor: [^{3}H]nicotine as an agonist photoaffinity label. Biochemistry 1991;30:6987–97.
Mineur YS, Eibl C, Young G, Kochevar C, Papke RL, Gündisch D, et al. Cytisine-based nicotinic partial agonists as novel antidepressant compounds. J Pharmacol Exp Ther 2009;329:377–86.
Miyazawa A, Fujiyoshi Y, Unwin N. Structure and gating mechanism of the acetylcholine receptor pore. Nature 2003;423:949–55.
Moore MA, McCarthy MP. Snake venom toxins, unlike smaller antagonists, appear to stabilize a resting state conformation of the nicotinic acetylcholine receptor. Biochim Biophys Acta 1995;1235:336–42.
Ortells MO, Barrantes GE. Molecular modelling of the interactions of carbamazepine and a nicotinic receptor involved in the autosomal dominant nocturnal frontal lobe epilepsy. Br J Pharmacol 2002;136:883–95.
Pagán OR, Eterović VA, García M, Vergne D, Basilio CM, Rodríguez AD, et al. Cembranoid and long-chain alkanol sites on the nicotinic acetylcholine receptor and their allosteric interaction. Biochemistry 2001;40:11121–30.
Pedersen SE, Dreyer EB, Cohen JB. Location of ligand binding sites on the nicotinic acetylcholine receptor alpha-subunit. J Biol Chem 1986;261:13735–43.
Sanghvi M, Hamouda AK, Jozwiak K, Blanton MP, Trudell JR, Arias HR. Identifying the binding site(s) for antidepressants on the *Torpedo* nicotinic acetylcholine receptor: [^{3}H]2-Azidoimipramine photolabeling and molecular dynamics studies. Biochem Biophys Acta 2008;1778:2690–9.
Schild HO. p*Ax* and competitive drug antagonism. Br J Pharmacol 1949;4:277–80.
Shytle RD, Silver AA, Lukas RJ, Newman MB, Sheehan DV, Sanberg PR. Nicotinic receptors as targets for antidepressants. Mol Psychiatry 2002;7:525–35.

Author's personal copy

Smith GR, Sansom MSP. Molecular dynamics study of water and Na+ ions in models of the pore region of the nicotinic acetylcholine receptor. Biophys J 1997;73:1364–81.

Stouten PFW, Frommel C, Nakamura H, Sander C. An effective solvation term based on atomic occupancies for use in protein simulations. Mol Simul 1993;10:97–120.

Tetko IV, Gasteiger J, Todeschini R, Mauri A, Livingstone D, Ertl P, et al. Virtual computational chemistry laboratory – design and description. J Comput Aided Mol Des 2005;19:453–63.

Unwin N. Refined structure of the nicotinic acetylcholine receptor at 4 Å resolution. J Mol Biol 2005;346:967–89.

Yamakura T, Chavez-Noriega LE, Harris RA. Subunit-dependent inhibition of human neuronal nicotinic acetylcholine receptors and other ligand-gated ion channels by dissociative anesthetics ketamine and dizocilpine. Anesthesiology 2000;92:1144–53.

Yu Y, Shi L, Karlin A. Structural effects of quinacrine binding in the open channel of the acetylcholine receptor. Proc Natl Acad Sci USA 2003;100: 3907–12.